Journal of Environmental Chemical Engineering 13 (2025) 116135

Contents lists available at ScienceDirect

Journal of Environmental Chemical Engineering

journal homepage: www.elsevier.com/locate/jece

Preparation of hydrophilic PVDF membrane via blending with Fe_3O_4 nanoparticles and PVA for improved membrane performance in BTEX removal from wastewater

Ngozi Enemuo [a], Heidi Richards [a,*], Michael O. Daramola [b]

[a] Molecular Sciences Institute, School of Chemistry, University of the Witwatersrand, Private Bag X3, WITS, Johannesburg 2050, South Africa
[b] Department of Chemical Engineering, Faculty of Engineering, Built Environment and Information Technology, University of Pretoria, Hatfield, Pretoria 0028, South Africa

ARTICLE INFO

Keywords:
Biogenic-synthesized Fe_3O_4-NPs
PVDF membrane
PVA
Hydrophilic modifiers
BTEX

ABSTRACT

The recurring cases of the presence of organic contaminants, which include benzene, toluene, ethylbenzene, and xylene (denoted as BTEX) in our water bodies, have reaffirmed the need for continuous development of new strategies for proper BTEX wastewater treatment before discharge. In this study, biogenic-synthesized iron oxide nanoparticles (Fe_3O_4-NPs) and polyvinyl alcohol (PVA) were utilized as hydrophilic modifiers to mitigate the non-specific hydrophobic interaction of BTEX and polyvinylidene fluoride (PVDF) membrane to improve membrane performance. Chemical compositional analysis of the membrane confirmed that hydrophilic functional groups were infused into the membrane due to blending the Fe_3O_4-NPs and PVA into the PVDF membrane. The PVA-Fe_3O_4-PVDF membrane displayed improved hydrophilicity as indicated by its water contact angle (WCA) of 40.5°. Consequently, its anti-fouling performance was enhanced. The total fouling ratio (R_t) of the pristine PVDF was 0.48, of which 0.25 and 0.23 are irreversible (R_{ir}) and reversible (R_r) fouling, respectively. This was reduced to an R_t of 0.18 for the modified membrane, and the irreversible fouling declined to 0.02, while 0.16 of the fouling is reversible. The porosity of the modified membrane was also enhanced, resulting in the pure water flux of the membrane improving from 165.3 $Lm^{-2}h^{-1}$ (pristine membrane) to 313.7 $Lm^{-2}h^{-1}$ (modified membrane). With the Fe_3O_4-NPs acting as nanofillers in the modified membrane matrix, the enhanced membrane porosity did not adversely affect its rejection efficiency. The test of the stability of the modified membrane under long-term filtration revealed that the membrane has good and improved operational stability compared to the pristine membrane.

1. Introduction

The presence of harmful organic contaminants in our water bodies has constituted a significant environmental challenge that has intensified the need for the development of improved treatment strategies for effective treatment of contaminated water before discharge [1,2]. Such organic contaminants include benzene, toluene, ethylbenzene, and xylene (typically denoted as BTEX). Human exposure to BTEX-contaminated water could result in mild or severe health complications depending on many factors, which include the level of the BTEX in the water system, the method of exposure, and the duration of the exposure [3–6]. The aquatic organisms are also adversely impacted by BTEX water contamination as the exposed organisms could experience growth impairment, degenerative organ damage, and embryonic deformation, amongst others [7–10]. Moreover, the volatilization of the BTEX from the contaminated water body results in poor air quality in the surrounding atmosphere [6].

To address the health and environmental risks associated with BTEX water contamination, various methods have been developed for BTEX removal from the contaminated wastewater prior to discharge [11–13]. Among the treatment approaches, membrane technology offers a more efficient means of treatment of BTEX-contaminated water [14,15]. This is attributed to the ease of the membrane fabrication and application, low cost, minimal energy consumption, and low chances of generating secondary pollution during the treatment process[14,16,17]. Despite these remarkable attributes of membranes in organic wastewater

* Corresponding author.
E-mail address: heidi.richards@wits.ac.za (H. Richards).

https://doi.org/10.1016/j.jece.2025.116135
Received 6 September 2024; Received in revised form 14 February 2025; Accepted 9 March 2025
Available online 11 March 2025

treatment, their application is limited by the hydrophobicity of most membrane materials [18,19]. This is because of the hydrophobic interactions between the membranes and the organic contaminants during the treatment process, which results in membrane fouling and subsequent deterioration of the membrane performance [20,21].

To overcome this challenge, several strategies have been employed to suppress such hydrophobic interaction that occurs between the membranes and the organic contaminants to ensure long-term and sustainable membrane performance [20,22–25]. Among the membrane modification strategies is the incorporation of hydrophilic additives such as nanomaterials and hydrophilic polymers into the membranes [26–29]. The role of these additives as hydrophilic modifiers to resist membrane fouling is achieved through two main mechanisms: the forming of hydration layer and the steric repulsion effect [30].

Nanomaterials such as silver [18], titanium dioxide [31], zinc oxide [32], and iron oxide [33] nanoparticles have been extensively used as modifiers for many hydrophobic membranes due to their intrinsic hydrophilic properties. Another vital feature of nanomaterials that is key to their use in membrane modification is their nano size, which provides a large surface-to-volume ratio, thereby ensuring more efficient interaction of the particles with the membranes [34]. However, agglomeration of the nanomaterials in the matrix of the membranes remains a significant drawback to their use as membrane modifiers [35]. The agglomeration of the nanomaterials occurs due to their high surface energy, resulting in increased interaction between the nano-sized particles; hence, the amount of nanomaterials used in membrane modification is limited to low concentration to minimize such agglomeration [36]. Oftentimes, nanomaterials are biogenically synthesized to harness the capping ability of the biological extracts used in the synthesis and reduce their tendency to agglomerate [37,38]. Although such a method of nanomaterial preparation may not completely eliminate agglomeration, it greatly minimizes the agglomeration [37]. In addition, some compounds in the biological extracts, such as polyphenols, are rich in hydrophilic functional groups, which further contributes to the nanomaterials' hydrophilicity [39].

Hydrophilic polymers are another class of modifiers notably employed in endowing hydrophobic membranes with improved hydrophilicity [19]. Some of the most frequently utilized hydrophilic polymers in membrane modifications are polyethylene glycol (PEG) [40], polyacrylonitrile (PAN) [41], and polyvinyl alcohol (PVA) [42]. These polymers are endowed with hydrophilic functional groups; hence, these hydrophilic functional groups are introduced into a hydrophobic membrane during the modification process, thereby improving the membrane hydrophilicity. PVA, for instance, as a polyhydroxy, consists of many hydroxyl groups that are exploited to endow hydrophobic membranes with hydrophilic properties by coating or blending the PVA on the membrane [43,44].

To achieve optimal hydrophilic membranes, most research has focused on utilizing more than one hydrophilic modifier in the membrane modification [44–46]. Zuo et al. [47] utilized two hydrophilic modifiers, pyrogallol and polyethyleneimine, to improve the hydrophilicity of a PVDF membrane, subsequently improving the PVDF membrane performance in oil/water emulsion treatment. Similarly, Liu et al. [48] harnessed the hydrophilic properties of SiO_2 and PVA to boost the hydrophilicity and performance of a PVDF membrane for separating oil-in-water emulsion. For hydrophilic membrane modification specifically for the separation of BTEX from wastewater, very few studies have been done in this field. Saeedi-Jurkuyeh et al. [49] used graphene oxide and PEG to modify a polysulfone (PSF) membrane for the removal of two of the constituents of BTEX, benzene and toluene. Improved separation performance of the PSF membrane was attained after the modification under a short-term separation test [49]. Makhani et al. [50] modified a PES membrane utilizing a single hydrophilic modifier, tannin iron complex (TA-Fe^{III}), for BTEX separation. The PES membrane permeability and rejection were improved as a result of the modification; however, the rejection of some of the BTEX constituents was as low as 60 % due to the enlarged macro-voids of the membranes resulting from the agglomeration of the TA-Fe^{III} at high concentration [50]. Similarly, iron nanoparticles were utilized as a single modifier to enhance the performance of a PES membrane in treating BTEX wastewater [51]. However, the nanoparticles were agglomerated in the membrane matrix, especially at high concentrations, which reduced the expected impact of the Fe-Np on the membrane performance [51].

Owing to the very limited number of potential hydrophilic modifiers that have been studied for use in the hydrophilic membrane modification for the removal of BTEX from wastewater, it is vital that more hydrophilic modifiers be explored for this purpose. Biogenic-synthesized iron oxide nanoparticles (Fe_3O_4-NPs) are one of the potential hydrophilic modifiers that can be utilized for membrane modification. The incorporation of Fe_3O_4-NPs into the membrane is a low-cost and easy approach to membrane modification [52], and the extract of the plant used for the biogenic synthesis caps the Fe_3O_4-NPs and reduces their agglomeration [53]. Although the plant extract reduces the Fe_3O_4-NPs agglomeration, there is still a tendency for the NPs to agglomerate at very high concentrations [53]. Hence, the use of low concentrations of the NPs is necessary to prevent the NPs agglomeration. However, the low amount of the NPs is often insufficient to achieve a highly hydrophilic membrane. Thus, the incorporation of another hydrophilic modifier could be a viable means of further improving the hydrophilicity and separation performance of membranes. PVA is a low-cost hydrophilic polymer that can be used for hydrophilic modification of membranes. However, polymer incompatibility between the PVA and the membrane can occur at high concentrations of the PVA. Hence low concentration of PVA is ideal for achieving a stable polymer blend [54]. With the blending amounts of the two potential modifiers being limited, utilizing a hybrid of the ideal amounts of both modifiers could provide a cost-effective and easy approach to improve the hydrophilicity of membranes for treating BTEX wastewater.

This study explored the synergistic effect of blending biogenic-synthesized iron oxide nanoparticles (Fe_3O_4-NPs) and PVA into a PVDF membrane to mitigate the fouling tendency of the membrane during the BTEX wastewater treatment. Low concentrations of the Fe_3O_4-NPs and PVA were utilized for the membrane modification to minimize the NPs agglomeration or polymer incompatibility between PVDF and PVA. However, the combined effect of the two modifiers compensates for the low amount of the individual modifiers used to enhance the membrane's performance. The fouling resistance of the PVA-Fe_3O_4-PVDF membrane was investigated by performing antifouling tests with synthetic BTEX wastewater. Other performance tests were also conducted by measuring parameters such as pure water flux, BTEX flux, and rejection capacity of the membrane. The operational stability of the modified membrane was also studied. The features of the modified membrane were assessed using characterization techniques, which include Fourier transform infrared spectroscopy (FTIR), water contact angle, scanning electron microscopy (SEM), and atomic force microscopy (AFM). The stability of the modifiers in the membrane matrix was also assessed by performing leaching studies of the membrane.

2. Materials and methods

2.1. Materials

PVDF pellets (M_w ~ 180,000), PVA (M_w ~ 23,000), maleic acid, benzene (99.8 %), ethylbenzene (>99.9 %), toluene (99.9 %), and xylene (≥99 %), 1-methyl-2-pyrrolidinone (NMP) were bought from Sigma Aldrich. Deionized (DI) water (18.2 MΩcm @25 °C) used throughout this study was supplied from the millipore Direct-Q UV ultrapure water system. These reagents were used as they were received with no additional purification. Fig. 1

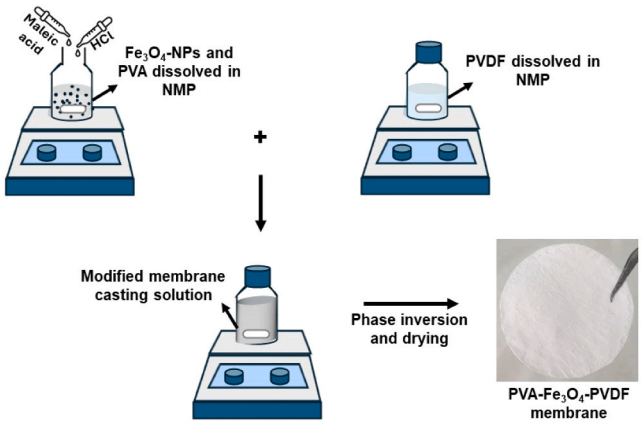

Fig. 1. The schematic diagram of the PVA-Fe_3O_4-PVDF membrane preparation process.

2.2. Preparation of the hydrophilic-modified membrane

The first step in the fabrication of the membrane was to select an ideal base membrane for treating the BTEX wastewater. PES and PVDF membrane casting solutions were prepared by dissolving 15 wt% of PES or PVDF in 85 wt% of NMP at 80 °C for 8 h under rigorous stirring, followed by casting the membranes using an immersion precipitation approach with water as the non-solvent. The suitability of the base membrane was assessed based on the membrane's tolerance to BTEX exposure. For this test, PES and PVDF membranes were immersed in 1000 ppm of BTEX water at 25 °C. The membranes were taken out of the BTEX water after being immersed for 30 days, then rinsed and dried in the oven at 40 °C. The tolerance of the membrane to the BTEX solution was inferred from the physical observation of the immersed membranes and their SEM images. As depicted in Fig. 2 of the results section, PVDF exhibited the best BTEX tolerance; hence, PVDF was chosen as a base membrane for the fabrication of the modified membrane.

The Fe_3O_4-NPs used for the membrane modification were biogenically synthesized, and the synthetic procedure was discussed in our previous work [55]. The amounts of the Fe_3O_4-NPs and PVA hydrophilic modifiers used to prepare the casting solution were carefully selected to ensure that the membrane structure and performance were not adversely affected due to NPs agglomeration or polymer incompatibility. From our previous work, a blending amount of 1 wt% Fe_3O_4-NPs was established as the optimum amount to achieve the well-dispersion of the Fe_3O_4-NPs in the PVDF membrane matrix [55]. Additionally, 0.1 wt% PVA was reported as the ideal amount to blend in a PVDF membrane to eliminate incompatibility between the two polymers [56]. Hence, 1 wt% of Fe_3O_4-NPs and 0.1 wt% of PVA were used to prepare the membrane casting solution. Other components in the casting solution for the modified membrane were 83.7 wt%, 15 wt%, 0.1 wt%, and 0.1 wt% of NMP, PVDF, maleic acid, and HCl, respectively. The casting solution was prepared by first obtaining a homogenous Fe_3O_4-NPs suspension by dispersing the Fe_3O_4-NPs in 1 mL of NMP and sonicating for 1 h. PVA was thoroughly dissolved in NMP, and the well-dispersed Fe_3O_4-NPs suspension was transferred into the PVA solution, which was then stirred for 3 h at 80 °C until a homogenous mixture of the Fe_3O_4-NPs and PVA was obtained. Maleic acid and HCl, used to initiate the crosslinking of the polymers, were then dropped into the mixture and stirred vigorously for 2 min. PVDF was thoroughly dissolved in NMP, added to the Fe_3O_4-NPs/PVA mixture, stirred for 3 h, sonicated for 30 min, and then stirred again for 1 h. The obtained casting solution was cooled and degassed to remove air bubbles and cast on a clean, smooth glass plate of an elcometer automatic film applicator. After a short while, the membrane cast film was immersed in a coagulation bath, DI water, for about 5 min to ensure the complete exchange of the NMP from the formed membrane. The membrane was then thoroughly rinsed with DI water and oven-dried at 40 °C for about 2 h.

For the pristine membrane, 15 wt% of PVDF was dissolved in 85 wt% of NMP at 80 °C for 8 h under rigorous stirring. The pristine membrane was then cast and dried using the same procedure described. It was then used as a control membrane to assess the features and performance improvement of the modified membrane.

2.3. Characterization of the membrane

The morphological properties of the modified and pristine membranes were analyzed using a high-resolution Carl Zeiss scanning electron microscope and WITec alpha300 atomic force microscope. The membranes for SEM cross-section analysis were stiffened by freezing in liquid nitrogen and carefully fractured. Energy-dispersive X-ray spectroscopy (EDX), performed on the same high-resolution Carl Zeiss scanning electron microscope, was employed to confirm that the Fe_3O_4-NPs were introduced into the membrane. Prior to the SEM analysis, all membranes were sputter-coated with Pd/Au and carbon using EmiTech K550X Sputtercoater for Pd/Au and EmiTech K950X Turboevaporator (Quorum Technologies, Lewes, England) for carbon.

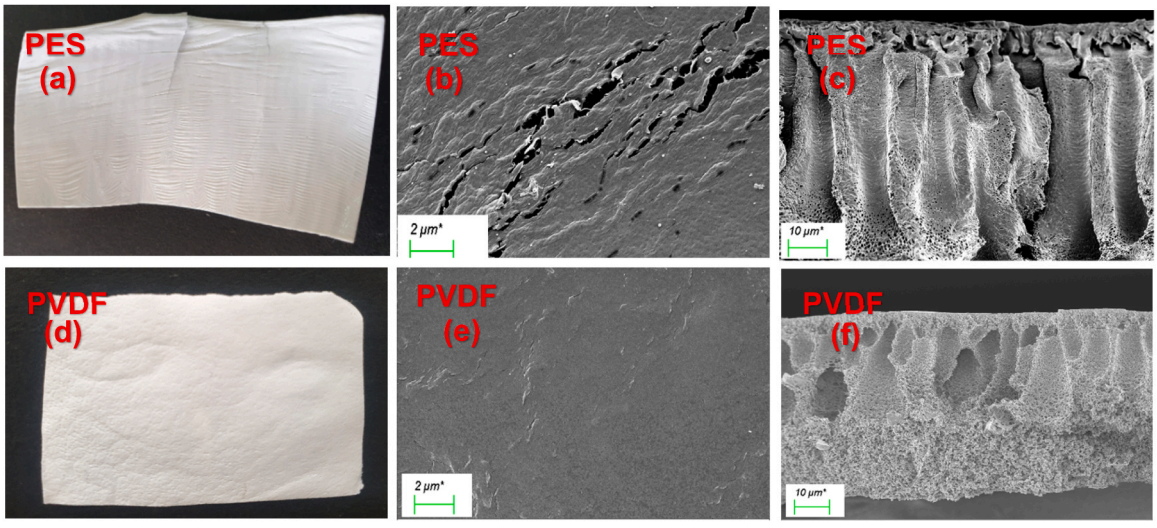

Fig. 2. The outcome of BTEX exposure of PES and PVDF membrane depicted by (a, d) photographs, (b, e) SEM image of membrane top surface, and (c, f) SEM image of membrane cross-section.

The compositional analysis of the membranes was performed with an FTIR Bruker Tensor 27 to confirm the successful introduction of the hydrophilic functional groups.

The membrane's hydrophilicity was tested by measuring their WCA employing the sessile drop method done on a goniometer G10, KRUSS. An average of five WCA measurements was reported. Membrane's hydrophilicity can also be stipulated by measuring their equilibrium water content (EWC) [57]. The EWC is also directly related to the porosity (ε) of membranes, and both parameters (EWC and porosity) can be obtained using the gravimetric method with the formula for their calculations shown in Eqs. (1) and (2). The W_{dry} and W_{wet} in the equations are the masses of the dry membrane and the wet membrane after being immersed in DI water for 48 h at room temperature, respectively.A, ρ, and$l$ in Eq. (2) is the membrane effective area (m^2), density of water (g/cm^3), and the membrane thickness (m), respectively. Water on the immersed membrane was wiped, and it was weighed immediately.

$$EWC(\%) = \left(\frac{W_{wet} - W_{dry}}{W_{wet}}\right) \times 100 \quad (1)$$

$$\varepsilon(\%) = \frac{(W_{wet} - W_{dry})}{\rho \times A \times l} \times 100 \quad (2)$$

The mean pore size (r_m) of the membranes was determined using the Guerout-Elford-Ferry equation shown in Eq. (3).

$$r_m = \sqrt{\frac{(2.9 - 1.75\varepsilon)8\eta lQ}{\varepsilon \times A \times \Delta P}} \quad (3)$$

Whereby ε (%), l (m), and A (m^2) denotes the porosity, thickness, and effective filtration area of the membrane, respectively. η denotes the viscosity of pure water (8.9×10^{-4} Pa.s), Q ($m^3\ s^{-1}$) represents the volume of water filtered per unit time and ΔP denotes the transmembrane pressure difference.

The membrane's surface charge was measured with a Malvern instrument Zetasizer Nano-ZS. The membrane was immersed in a 0.01 M, 300 mL KOH electrolyte solution for 2 days at pH ranging from 1.8 to 11.7, with the required solution pH adjusted by dosing with a dilute HCl or NaOH. The soaked membrane was sliced and inserted into a custom dip cell, which was immersed in a solution of the background electrolyte.

The membrane's thermal stability was determined under nitrogen between 25 °C and 800 °C at a heating rate of 10 °C/min using a TA SDT Q600 thermogravimetric analyzer. XT plus TA Tesla analyzer was used to test the membrane's mechanical properties.

2.4. Membrane performance evaluation

Synthetic BTEX water was utilized in the study because of the challenges in acquiring industrial wastewater containing BTEX contaminants. The concentration of each of the contaminants in the feed solution, that is, benzene, toluene, ethylbenzene, and xylene, was 100 ppm, which is above their reported environmental level [58,59]. The synthetic BTEX water was prepared by dissolving the contaminants and then shaking the solution at room temperature for 6 h. The short-term filtration and BTEX rejection tests were performed utilizing a Sterlitech HP4750 dead-end stirred cell. Prior to the tests, the membrane was compacted for 30 min using DI water at a transmembrane pressure (TMP) of 350 kPa to attain a steady flux. The flux and separation tests were conducted at a TMP of 300 kPa with DI water and BTEX water. The pure water flux (PWF) and BTEX flux were calculated according to Eq. (4).

$$J = \frac{V}{A \times \Delta t} \quad (4)$$

J represents the PWF or BTEX flux (L/m^2h), V denotes the permeate volume (L), A denotes the effective filtration area of the tested membrane (m^2), and Δt is the permeation time (h).

BTEX rejection capacity of the membranes was obtained by filtering the BTEX water through the membrane under constant stirring of the feed solution at 300 kPa and room temperature. A gas chromatograph instrument, Agilent 7890 A (column: 30 m × 0.25 mm ID BP5MS × 0.25 μm) with a flam6e ionization detector (FID), coupled with an automatic liquid sampler (Agilent 7693 A) was utilized to measure the BTEX concentration in the permeate. A constant flow rate of the mobile phase (nitrogen gas) was maintained at 2.64 mL/min, with a 0.2 μL injection volume in a splitless mode. The oven initial temperature was set and held at 40 °C for 2 min, followed by ramping to 90 °C and held for 3 min at 10 °C/min, and lastly to 200 °C and held for 2 min at 20 °C/min. Eq. (5) was used to calculate BTEX percentage rejection.

$$R \quad (\%) = \frac{C_f - C_p}{C_f} \quad (5)$$

C_f and C_p are, respectively, the BTEX concentration (ppm) in the BTEX feed solution and the permeate.

The effect of the hydrophilic modifiers on improving the membrane's fouling resistance was assessed by performing antifouling tests. For this test, the PWF of the membrane was obtained for 3 h at 300 kPa, followed by the filtration of BTEX solution for 3 h at the same TMP. The membrane was subsequently cleaned by washing and backwashing with DI water for 1 h and ultrasonically for another 30 min. The PWF of the cleaned membrane was assessed for 3 h filtration. The fouling resistance of the membrane was determined by calculating the reversible fouling ratio (R_r), irreversible fouling ratio (R_{ir}), the total fouling ratio (R_t), and the flux recovery ratio (FRR) were then calculated according to Eqs. (6)–9), respectively. The membrane cleaning efficiency (η_c) was also calculated using Eq. (10).

$$R_r = \frac{J_C - J_{BTEX}}{J_w} \quad (6)$$

$$R_{ir} = \frac{J_w - J_C}{J_w} \quad (7)$$

$$R_t = R_r + R_{ir} \quad (8)$$

$$FRR = \frac{J_C}{J_w} \quad (9)$$

$$\eta_c = \left(\frac{J_C - J_{BTEX}}{J_W - J_{BTEX}}\right) \quad (10)$$

Where J_w is the first PWF, J_{BTEX} denotes the flux of the BTEX feed solution while J_C represents the membrane PWF obtained after cleaning.

The stability of the membrane in terms of its operational stability and the stability of the incorporated modifiers in the membrane matrix was investigated. For operational stability, the flux and rejection capacity of the membrane, under the same parameters described above, were studied for a longer period using a crossflow filtration system, Sterlitech membrane test system. The procedure involves the filtration of the synthetic BTEX feed water through the membrane for 120 h, with filtrate samples collected every 6 h. To assess the stability of the modifiers in the membrane matrix, the permeates were analyzed with an inductively coupled plasma mass spectrometer (ICPMS), PerkinElmer Inc., to obtain the iron concentration in the filtrate, which was utilized to infer the leaching tendency of the Fe_3O_4-NPs from the membrane. The morphology and chemical composition of the used membrane were also obtained using SEM and FTIR to determine any morphological or compositional changes due to the leaching of the incorporated modifiers.

3. Results and discussion

3.1. Fe_3O_4-NPs characterization

The identification, chemical composition, morphology, and textural properties of the biogenic-synthesized Fe_3O_4-NPs were extensively discussed in our previous work [55].

3.2. Selection of the base membrane

Fig. 2 presents the images of the PES and PVDF membrane materials exposed to BTEX water. As seen in Fig. 2(a), there was some damage to the PES membrane after being exposed to the BTEX water, as the membrane became a little flaky. The damage is further confirmed by the crackiness on the membrane, as shown in the SEM image of the membrane surface in Fig. 2(b). However, the inner structure of the PES membrane did not change after being exposed to the BTEX water, as presented in Fig. 2(c). On the other hand, the PVDF membrane displayed excellent BTEX tolerance, as seen in all the images (Fig. 2(d)–(f)) of the membrane after its exposure to the BTEX water. Due to the outstanding tolerance of PVDF to BTEX water, PVDF was adopted as the ideal base membrane for application in the BTEX water treatment.

3.3. Membrane chemical composition

The blending of PVA into the PVDF membrane was confirmed by the FTIR spectra depicted in Fig. 3. The pristine PVDF membrane shows peaks at 679 cm^{-1} and 762 cm^{-1}, which emanate from the functional group of CF_2 chemical bonds, and the peaks at 1180 cm^{-1} and 1072 cm^{-1} originate, respectively, from the asymmetric stretching and symmetric stretching of -CF_2 [60,61]. The peak for CH deformation appeared at 1401 cm^{-1}, and other peaks at 873 cm^{-1} and 832 cm^{-1} are linked to the C-C-C bonds of the PVDF membrane [62]. For the PVA, the broad peak seen at 3288 cm^{-1} represents the O-H stretching. Other peaks at 2934, 2905, 1416, 1323, 1138, 1083, 916, and 829 cm^{-1} are due to asymmetric stretching of CH_2, symmetric stretching of the CH_2, the bending of CH_2, OH rocking with the CH wagging, the shoulder stretching of the C-O, stretching of C═O and bending of OH, rocking of CH_2, and C-C stretching respectively [63]. Comparing the spectra of the pristine PVDF membrane with the spectra of the PVA-Fe_3O_4-PVDF membrane, there were obvious peak changes resulting from the modification. For instance, unlike the pristine membrane, the PVA--Fe_3O_4-PVDF membrane exhibited a broad peak at 3288 cm^{-1}, ascribed to O-H stretching, thus establishing the presence of the hydrophilic hydroxyl group in the modified membrane. Additionally, there were peak changes in the region between 1272 cm^{-1} and 1033 cm^{-1} which originates from the entanglement of the molecular chains of PVDF and PVA, thus confirming the integration of the two polymers.

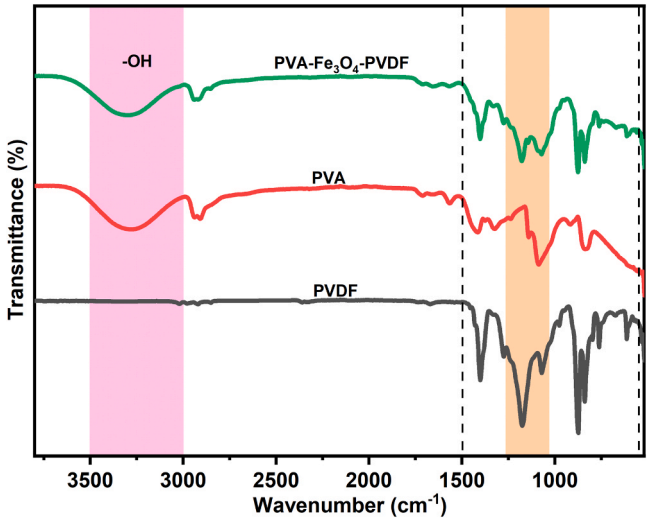

Fig. 3. FTIR spectra of PVDF, PVA, and PVA-Fe_3O_4-PVDF.

3.4. Membrane morphology

SEM images of the modified and pristine membranes, as Fig. 4 shows, revealed the impact of the modifiers on the surface and inner morphology of the membrane. The pristine membrane's surface was smooth and less porous, while the PVA-Fe_3O_4-PVDF membrane had a rougher and more porous surface, as shown in Fig. 4(a) and (d). This observed change on the PVA-Fe_3O_4-PVDF membrane surface shows that the incorporation of the modifiers accelerated the demixing process during the phase inversion because of the hydrophilic nature of the modifiers. Hence, the better hydrophilicity of the modified membrane cast solution necessitated a fast solvent-nonsolvent exchange, resulting in the formation of a more porous membrane structure.

Comparing the cross-section morphology of the two membranes also indicates that the addition of the modifiers increased the rate of diffusion of the non-solvent (DI water) into the membrane during the phase inversion. This is established from the difference in the formed finger-like pores in the membranes. As depicted in Fig. 4(b), the finger-like pores of the pristine membrane were shorter, while the finger-like pores of the PVA-Fe_3O_4-PVDF membrane, shown in Fig. 4(f), were longer. With the incorporated hydrophilic modifiers, the membrane solution had more affinity for water; hence, on immersing the casted membrane into the coagulation bath, the diffusion of water into the membrane was faster. This results in the forming of longer finger-like pores in the modified membrane, which is anticipated to enhance the flux of the membrane but may negatively affect its BTEX rejection efficiency. The concern about the possible reduced rejection capacity of the modified membrane due to its enhanced pore structure was addressed by the presence of the Fe_3O_4 nanoparticles in its matrix, as shown in the higher magnification image of the membrane in Fig. 4(g) and Fig. 4(h). The role of the Fe_3O_4 nanoparticles as nanofillers is evident in the images, and it will be significant in ensuring that the membrane's rejection capacity is not notably compromised by the longer macropores of the modified membrane.

The Fe_3O_4-NPs in the modified membrane were not agglomerated but well dispersed throughout the membrane, as depicted in Fig. 4(g) and (h); thus, all the expected attributes of the Fe_3O_4-NPs would be maximized in improving the membrane's properties and its performance.

Morphological interpretation in terms of the membrane surface roughness was obtained using AFM analysis of the membrane, and the roughness images are presented in Fig. 5. The average roughness (Sa) of the pristine PVDF membrane was 44.2 nm, and its root mean square roughness (Sq) was 48.6 nm. On adding the modifiers to the membrane, the Sa increased to 59.3 nm while the Sq increased to 62.8 nm. This revealed that the modification of the PVDF membrane using the Fe_3O_4-NPs and PVA significantly enhanced the membrane surface roughness. According to Wenzel's model, the roughness of a surface influences its wettability, with a rougher surface exhibiting higher wettability and vice versa [64]. Thus, the improved surface roughness of the PVA--Fe_3O_4-PVDF membrane could be beneficial in enhancing the wettability of the membrane, which consequently results in improved membrane permeability. In addition, the rougher membrane surface provides more membrane area, which also favours the membrane permeability.

3.5. Membrane hydrophilicity, equilibrium water content, porosity and mean pore size

The impact of the modifiers on the membrane's hydrophilicity was analyzed using the sessile drop WCA measurements, and the result is shown in Fig. 6(a). On incorporation of the modifiers into the PVDF, the

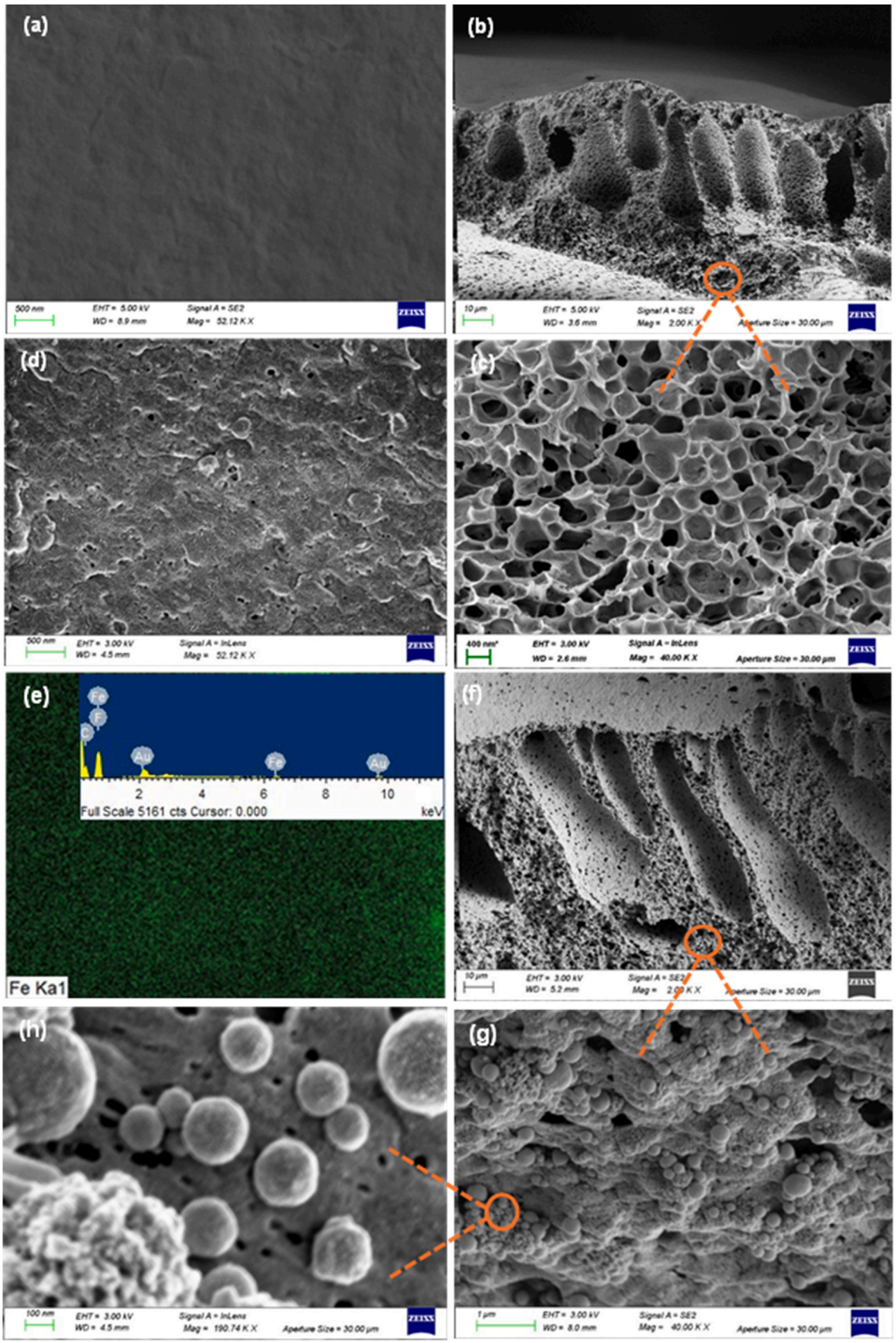

Fig. 4. SEM image of the (a) surface of pristine membrane, and inner structure of pristine membrane at magnification (b) 2.00 KX, and (c) 40.00 KX, (d) surface of PVA-Fe_3O_4-PVDF membrane, (e) EDX mapping image of PVA-Fe_3O_4-PVDF, and the inner structure of PVA-Fe_3O_4-PVDF at magnification (f) 2.00 KX, (g) 40.00KX, and (h) 190.74KX.

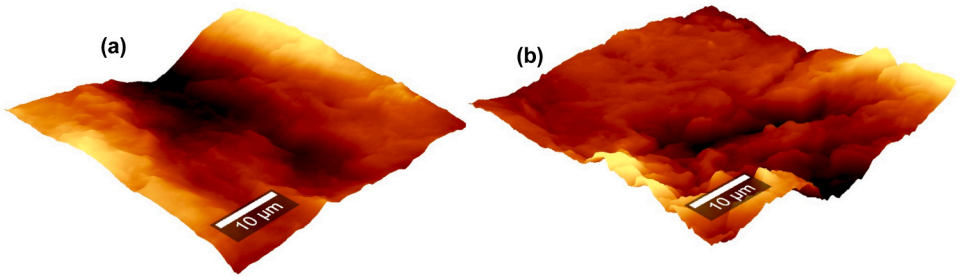

Fig. 5. AFM images of the (a) pristine membrane, and (b) PVA-Fe_3O_4-PVDF membrane.

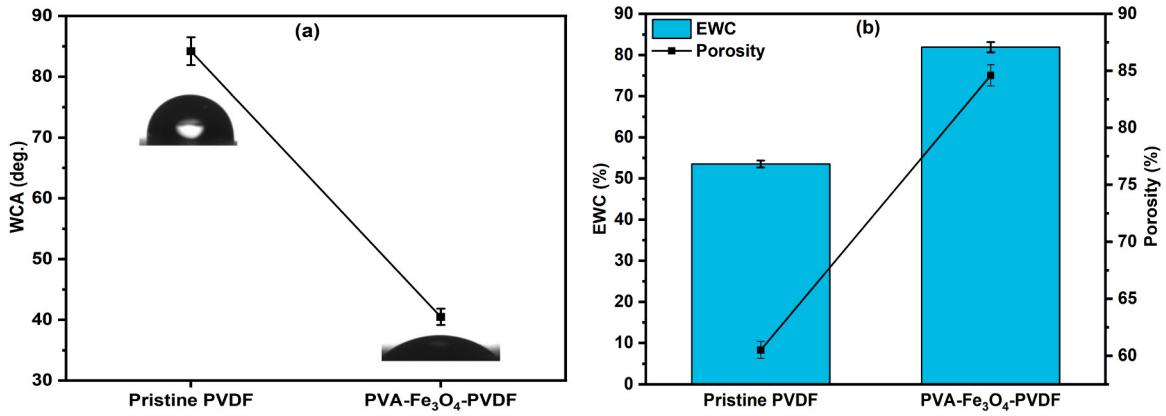

Fig. 6. (a) WCA, and (b) EWC and porosity of the pristine PVDF and PVA-Fe_3O_4-PVDF membrane.

WCA of the membrane decreases from 84.2° to 40.5°, which signifies an improvement in its hydrophilicity. This is due to the hydrophilic nature of the two modifiers embedded into the membrane. Iron oxide nanoparticles are intrinsically hydrophilic, and their high surface area to volume ratio ensures good transfer of the hydrophilic property to the membrane [36,65].

The other modifier, PVA, is composed of hydroxyl groups, which are highly hydrophilic functional groups [66]. This hydrophilic feature of the PVA is incorporated into the PVDF membrane, thereby contributing to improving the modified membrane's hydrophilicity. Thus, the synergistic effect of the hydrophilic nature of the two modifiers bestowed the modified membrane with improved hydrophilicity. With such enhanced hydrophilicity, the membrane surface can form a stable hydration layer with the water molecules during the filtration process [67,68]. This is beneficial in promoting water permeation through the membrane and also reducing the rapid deposition of organic foulants on the membrane [69].

The membrane's equilibrium water content (EWC) is shown in Fig. 6 (b), and it further establishes that the PVA-Fe_3O_4-PVDF membrane's hydrophilicity was improved by incorporating the modifiers into the membrane. Compared with the pristine PVDF membrane, the PVA-Fe_3O_4-PVDF membrane has a 53 % increase in its EWC, which indicates a significant improvement in the membrane's affinity for water. The EWC is also governed by the porosity of a membrane [70], and the result of the membrane's porosity, also depicted in Fig. 6(b), shows that the porosity of the membrane increased from 60.5 % (pristine PVDF) to 84.6 % (modified membrane). This correlates with the increment observed in the EWC and the enhanced finger-like pores seen in the SEM image, Fig. 4(f) of the PVA-Fe_3O_4-PVDF membrane. The improvement in the membrane's porosity is due to the fast liquid-liquid exchange during the phase inversion, induced by the modifiers' presence, as explained in Section 3.4. Similarly, an increment in the mean pore size of the modified membrane was obtained, with the pristine membrane exhibiting a mean pore size of 40.3 nm while the modified membrane has a mean pore size of 60.9 nm. The observed increment is governed by the same phenomena of the fast demixing process during the phase inversion due to the presence of the hydrophilic modifiers, as previously illustrated in Section 3.4.

3.6. *Membrane surface charge, thermal and mechanical stability*

The surface charge of a membrane is one of the major determinants of its performance because the electrostatic interaction between a membrane and the contaminants influences the membrane's behaviour, such as its fouling phenomenon and separation efficiency [71]. Zeta potential measurements are often employed to measure the membrane surface charge, and this is performed at various pH since the membrane's surface charge depends on the solution's pH [72]. Fig. 7(a) shows the zeta potential values of the pristine PVDF and PVA-Fe_3O_4-PVDF membranes measured over a pH range of 1.8–11.7. At low pH between 1.8 and 4.0, both membranes have positive zeta potentials, however, the zeta potentials of the PVA-Fe_3O_4-PVDF membrane were less positive than that of the pristine PVDF membrane at this pH range. In addition, the modified membrane has an isoelectric point (IEP) of 4.09, while that of the pristine membrane was detected at 4.3. The protonation of the membranes' surface groups could explain their positive zeta potentials at low pH. With the modified membrane having a more oxygen-containing group on its surface, more H^+ is required to neutralize the surface negative charge and achieve a point of zero charge, hence the less positive zeta potential and IEP obtained for the modified membrane at this range. As the pH was further increased, the zeta potentials of both membranes changed to negative, with the modified membrane exhibiting more negative values. This is attributed to the deprotonation of the membranes' surface groups at higher pH, as well as the presence of more oxygen-containing groups in the modified membrane, which is also responsible for its observed higher negative zeta potential. This result of the zeta potentials of the modified membrane is imperative in predicting or understanding its behaviour in the

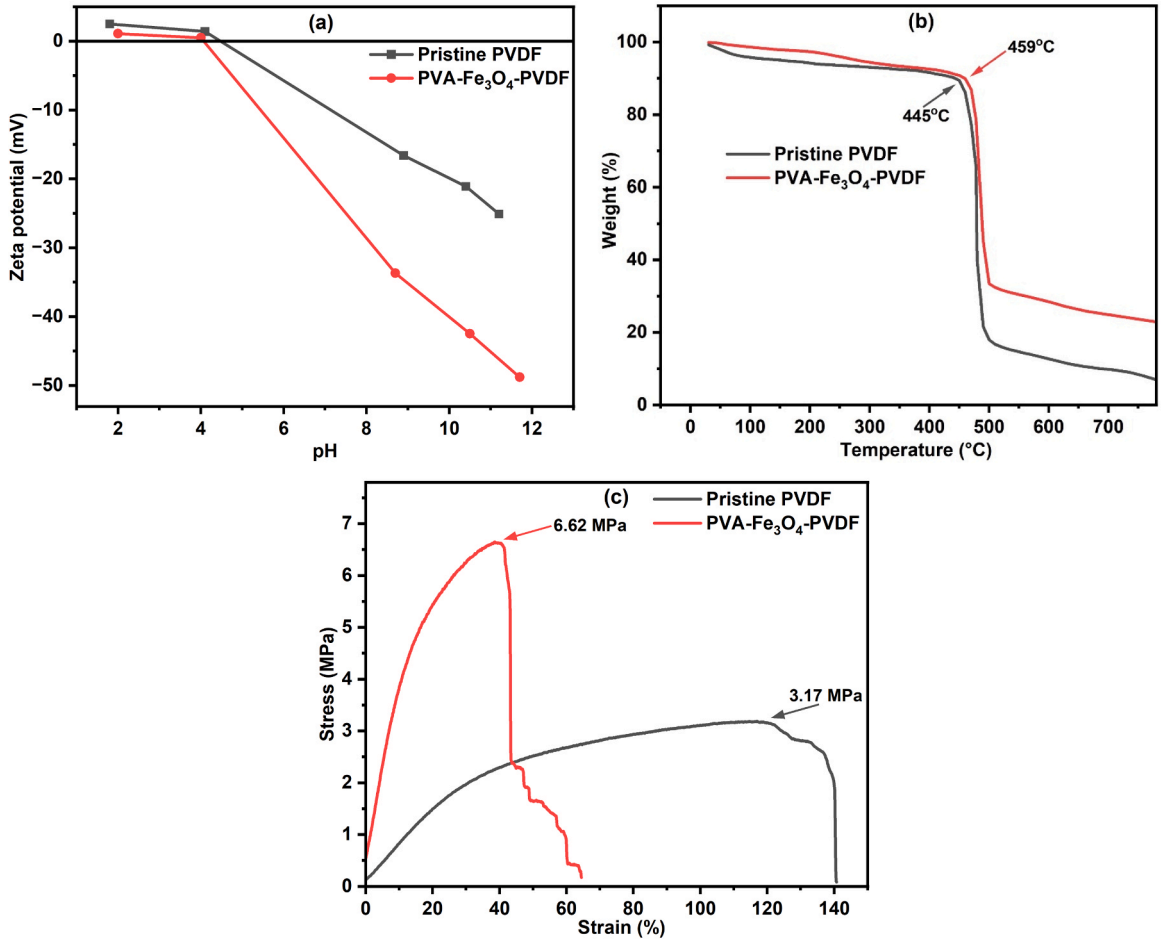

Fig. 7. (a) surface zeta potentials, (b) TGA curves, and (c) stress-strain curves of the pristine PVDF and PVA-Fe_3O_4-PVDF membrane.

treatment of BTEX wastewater at any of the studied pH.

Fig. 7(b) depicts the TGA curves of the membranes, which represent the modifiers' effect on the modified membrane's thermal stability. The pristine PVDF started to decompose at 445 °C owing to the good thermal stability of the polymer itself, and the PVA-Fe_3O_4-PVDF membrane began to decompose at 459 °C. This positive shift of the modified membrane's TGA curve signifies that the membrane's thermal stability was enhanced by incorporating the modifiers in the membrane. A plausible explanation for the improvement in the modified membrane's thermal stability is that there was good interaction and binding between the Fe_3O_4-NPs, PVA, and PVDF, which reinforced the membrane's molecular chain. In addition, the PVA-Fe_3O_4-PVDF membrane exhibited a one-step degradation process, which indicates that there was good entanglement of the molecular chains of the PVA and PVDF, thereby suggesting that the blend amounts of the two polymers used for the membrane fabrication produced a compatible polymer blend.

There was also an improvement in the mechanical strength of the PVA-Fe_3O_4-PVDF membrane, as illustrated by its stress-strain curve in Fig. 7(c). With the incorporation of the modifiers into the PVDF matrix, the ultimate tensile strength increased from 3.17 MPa (pristine membrane) to 6.62 MPa (modified membrane). Thus, its mechanical strength was doubled. This improved mechanical feature of the PVA-Fe_3O_4-PVDF membrane can be ascribed to the good mechanical stability of the Fe_3O_4-NPs [53], and the efficient entanglement of the molecular chains of the PVA and PVDF during the fabrication process. Besides, the biogenic-synthesized Fe_3O_4-NPs have oxygen-containing groups, such as hydroxyl, on its surface, as shown in its FTIR result [55]. The interaction of the hydroxyl group of the biogenic-synthesized Fe_3O_4-NPs and the PVA with the methyl group of the PVDF contributed to the enhanced mechanical property of the modified membrane. Ultimately, the synergistic impact of both modifiers resulted in the notable improvement of the modified membrane's ultimate tensile strength. Thus, the modified membrane can withstand more stress during its usage with such an improved mechanical strength. Conversely, the elongation tendency of the PVA-Fe_3O_4-PVDF membrane was reduced to about half when compared to that of the pristine membrane, as indicated by the reduced tensile strain of the PVA-Fe_3O_4-PVDF membrane. This decline in the tensile strain of the modified membrane could be directly linked to the improved rigidity introduced into the membrane by the Fe_3O_4-NPs, as well as the restraining of the molecular chains of the membrane due to the entanglement of the PVA and PVDF. These effects of the modifiers on the membrane limit its stretching ability, resulting in the observed decline in the membrane's tensile strain.

3.7. Permeance flux, separation, and antifouling performance of the membrane

The short-term permeation, separation, and antifouling performance of the modified membrane was investigated using a dead-end stirred filtration cell. Filtration was performed for 180 min using DI water or synthetic BTEX water to determine the membrane's PWF or BTEX flux. Fig. 8(a) shows that the PWF of the pristine membrane was 165 L/m^2h while that of the PVA-Fe_3O_4-PVDF membrane was 313 L/m^2h, which signifies that the PWF of the modified membrane was nearly doubled. This improvement can be linked to the enhanced hydrophilicity and pore structure of the modified membrane, as previously discussed. With the modified membrane being more hydrophilic and exhibiting better pore structure, it has more affinity for water, and the water permeation

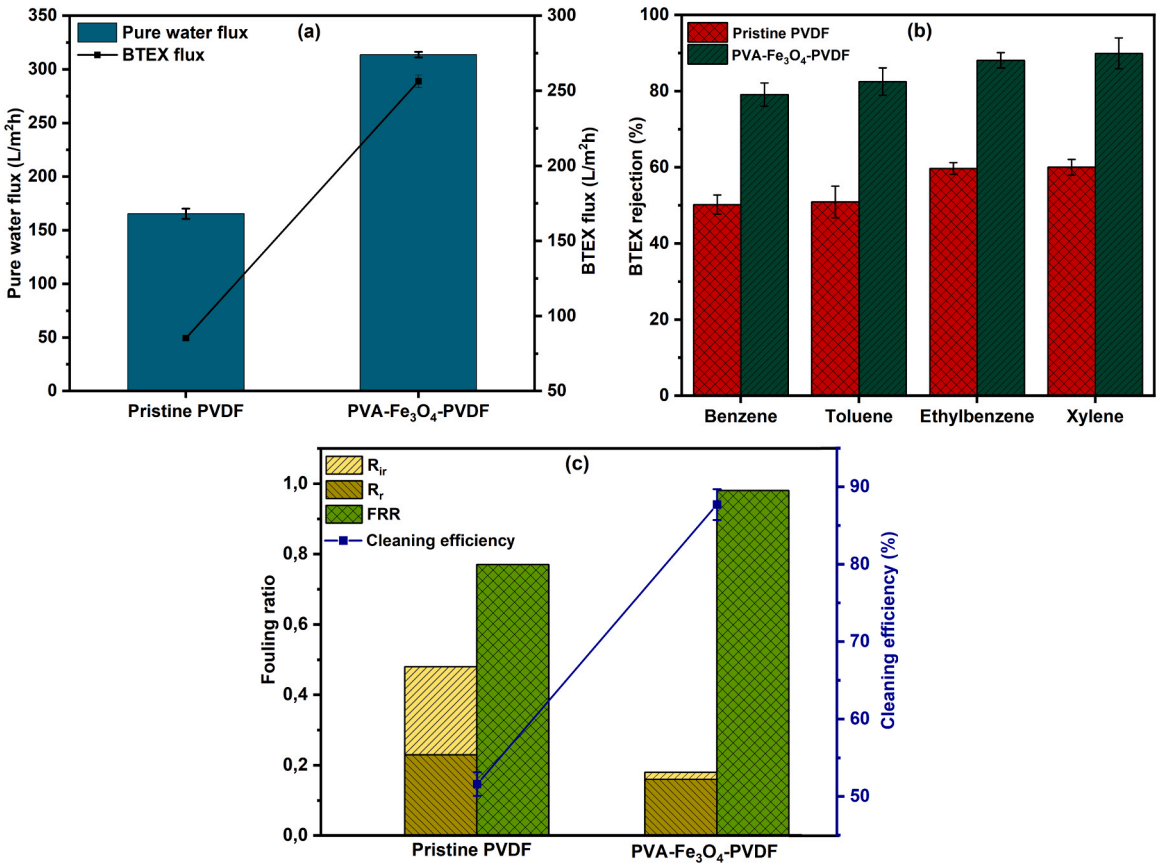

Fig. 8. (a) Permeate fluxes, (b) BTEX rejections, and (c) fouling ratios and cleaning efficiency of the membranes.

resistance was reduced.

On filtering the synthetic BTEX water through the membranes, a reduced flux was obtained compared with their counterpart PWF. The pristine membrane has a BTEX flux of 85 L/m^{2}h, and the BTEX flux of the PVA-Fe_3O_4-PVDF membrane was 256 L/m^{2}h. However, the modified membrane has a lesser flux decline of 18 % while the reduction in flux for the pristine membrane was 48 %. Formation of the hydration layer is a known phenomenon that occurs on the hydrophilic membrane surface during filtration, and it limits the adsorption of organic contaminants on the membrane [73], thus, the lesser flux decline seen with the modified membrane could be ascribed to the formation of the hydration layer on the membrane's surface, which minimizes BTEX adsorption on the membrane, resulting in the lesser flux reduction during the BTEX water filtration. There may have been an initial deposition of the BTEX contaminants on the membrane before a stable hydration layer was formed on the membrane's surface, and this explains the decline in the BTEX flux of the PVA-Fe_3O_4-PVDF membrane compared with its PWF.

An improvement in the BTEX rejection was also observed for the PVA-Fe_3O_4-PVDF membrane, as presented in Fig. 8(b). The hydration layer that formed on the surface of the hydrophilic-modified membrane prevented the BTEX contaminants from reaching and penetrating through the surface of the membrane, while few of the contaminants were deposited on the membrane before a stable hydration layer was formed. Hence, the improvement in the modified membrane BTEX rejection. Besides, the BTEX rejection was observed to increase in the sequence of benzene<toluene<ethylbenzene<xylene, thereby suggesting that some of the BTEX contaminants that reached the membrane could have been separated by size exclusion. The inference is justified by the fact that the molecular diameter of benzene (B) is 0.58 nm, toluene (T) is 0.60 nm, Ethylbenzene (E) is 0.63 nm, and Xylene (X) is 0.63 nm [74], and the rejection trend seemingly tallies with the molecular size of the BTEX contaminants. Therefore, it is postulated that the hydration layer and steric exclusion are the major separation routes that facilitated the removal of the BTEX using the modified membrane.

Fig. 8(c) presents the antifouling performance of the PVA-Fe_3O_4-PVDF membrane. Compared with the pristine membrane, there was a considerable improvement in the ability of the PVA-Fe_3O_4-PVDF membrane to suppress the non-specific adsorption of the organic BTEX contaminants on the membrane, as indicated by its lesser total fouling ratio, R_t. The membrane's R_t is the summation of its reversible fouling (R_r) and irreversible fouling (R_{ir}) ratio, and the modified membrane exhibited an R_t of 0.18, of which the R_r was 0.16 while the R_{ir} was 0.02. The R_t of the pristine PVDF membrane was 0.48, of which the R_r was 0.23, and the R_{ir} was 0.25. Thus, the antifouling propensity of the membrane improved by about 62.5 % with the addition of the modifiers to the membrane. The formation of a hydration layer as a result of improved hydrophilicity of the modified membrane created a barrier between the BTEX and membrane, thereby limiting the attachment of the BTEX contaminants to the membrane. When fouled, there was better ease of removing the foulants on the modified membrane through physical cleaning as indicated by its lesser R_{ir} of 0.02, compared with the R_{ir} of 0.25 for the pristine membrane. This is further established by the higher cleaning efficiency, η_c, of the modified membrane, which was found to have improved by 70 % through physical cleaning using water and ultrasonic agitation of the membrane. This antifouling result can be used to make a conclusive inference that, under short-term filtration, the modified membrane can significantly resist fouling from BTEX contaminants which invariably enhances the membrane's performance.

3.8. *Crossflow filtration performance*

The long-term filtration performance of the PVA-Fe_3O_4-PVDF membrane was tested using a crossflow system to determine its

operational stability in terms of the climax or limits of the membrane in regards to its BTEX flux, BTEX rejection, and reusability. Before these parameters were tested, the first crossflow experiment was conducted to determine that a stable PWF was attained after compacting the membrane for 2 h. Fig. 9(a) depicts the PWF of the membrane after compaction, which shows that the PWF remained relatively constant throughout the 18 h filtration of DI water. Hence, any decline in BTEX flux in the subsequent BTEX filtration could be attributed to membrane fouling, as the attachment of foulants on membranes results in a decline in their permeability [75].

Fig. 9(b) shows the BTEX flux of the membrane over a 120 h filtration, which indicates that the modified membrane maintained moderately the same BTEX flux for the first 84 h during the crossflow filtration, after which a steep decline in the BTEX flux is observed. This contradicts the performance of the pristine membrane, whose BTEX flux started declining from the initial stage of the filtration. The ability of the modified membrane to maintain its BTEX flux for 84 h could be ascribed to the formation of the hydration layer on the surface of the membrane, which prevented BTEX deposition on the membrane. However, after 84 h of filtration, the feed solution might have been more saturated, resulting in more BTEX breaking through the hydration layer and depositing on the membrane. This led to blockage or narrowing of the membrane's pores by the BTEX and, consequently, a decline in flux.

The modified membrane maintained fairly stable and high BTEX rejection throughout the long filtration process, with a slight decline in rejection as the filtration progressed, as shown in Fig. 10 (a–d). Considering that the rejection capacity of the PVA-Fe_3O_4-PVDF membrane was higher than that of the pristine membrane for the entire duration, the role of the hydration layer in forming an extra separation barrier on the surface of the PVA-Fe_3O_4-PVDF membrane is further established. Thus, while the pristine membrane might have removed the BTEX through only adsorption and steric exclusion, the modified membrane used the hydration layer on its surface as an extra barrier to achieve higher rejection. However, due to the saturation of the feed with time, the BTEX may break through the hydration layer, which results in the slight decline in rejection with time.

The reusability of the membrane after being subjected to long-term use was assessed by physically cleaning the membrane and subjecting the cleaned membrane to subsequent cycles of long-term BTEX filtration. The cleaning of the membrane was done by washing and backwashing with DI water for 1 h and mild ultrasonication for another 30 min. As presented in Fig. 11, the BTEX flux of the PVA-Fe_3O_4-PVDF membrane in the first cycle started at 258 L/m^2h, while the flux in the second cycle, after cleaning, started at 224 L/m^2h, which indicates that there was a 13 % decline in membrane's BTEX flux after performing physical cleaning of the membrane after long-term use. The decline in BTEX flux of the pristine membrane was obtained to be 47 %, thus implying that the modified membrane has a lesser BTEX flux decline than the pristine membrane. A similar trend in BTEX flux decline was observed for the modified and pristine membranes in the subsequent cycles. BTEX adsorption on the pristine membrane made its physical cleaning less effective in removing the adsorbed BTEX, while the modified membrane had less adsorbed BTEX because of the formation of a hydration layer that reduced BTEX adsorption on the membrane. Hence, physical cleaning of the modified membrane was more effective, although the 13 % BTEX flux decline shows that there is irreversible fouling that would require chemical cleaning. In addition, the PVA-Fe_3O_4-PVDF membrane fairly maintained its BTEX flux at the initial stage of each filtration cycle. For instance, the modified membrane exhibited relatively same BTEX flux until 84 h, 66 h, 66 h, and 54 h in filtration cycle 1, cycle 2, cycle 3, and cycle 4, respectively, before the observed decline in flux as depicted in Fig. 11. Meanwhile, the pristine membrane showed a rapid decline in BTEX flux from the onset of each filtration cycle. Hence, the hydration layer on the surface of the modified membrane minimized the BTEX deposition on the membrane, as previously discussed, thereby prolonging its reusability in BTEX water treatment.

Overall, the results of the long-term assessment of the membrane performance showed that the modified membrane has fairly good operational stability in the treatment of BTEX-contaminated wastewater.

3.9. Stability of the modifiers in the membrane matrix

The leaching of the Fe_3O_4-NPs from the modified membrane during wastewater filtration could constitute secondary contamination of the treated water and even reduce the membrane separation performance [76]. Thus, the stability of the Fe_3O_4-NPs in the matrix of the membrane was ascertained by performing the iron leaching test by measuring the concentration of iron in the filtrates collected during the long-term filtration tests. The results indicate that the concentration of iron in the filtrates was lower than 50 ppb. Although the World Health Organization (WHO) did not provide a definitive guideline value for the acceptable limit of iron in drinking water, it stated that a concentration of about 2 ppm and below poses no health risk [77]. Hence, the results of the iron leaching test suggest that the amount of iron in the filtrate is way below the amount that could be of any health risk. This implies that the incorporated Fe_3O_4-NPs were fairly stable in the membrane matrix thereby indicating that the use of this modifier to improve the PVDF membrane poses no health concerns that could emanate from its leaching.

Fig. 12(a) presents the SEM image of the PVA-Fe_3O_4-PVDF

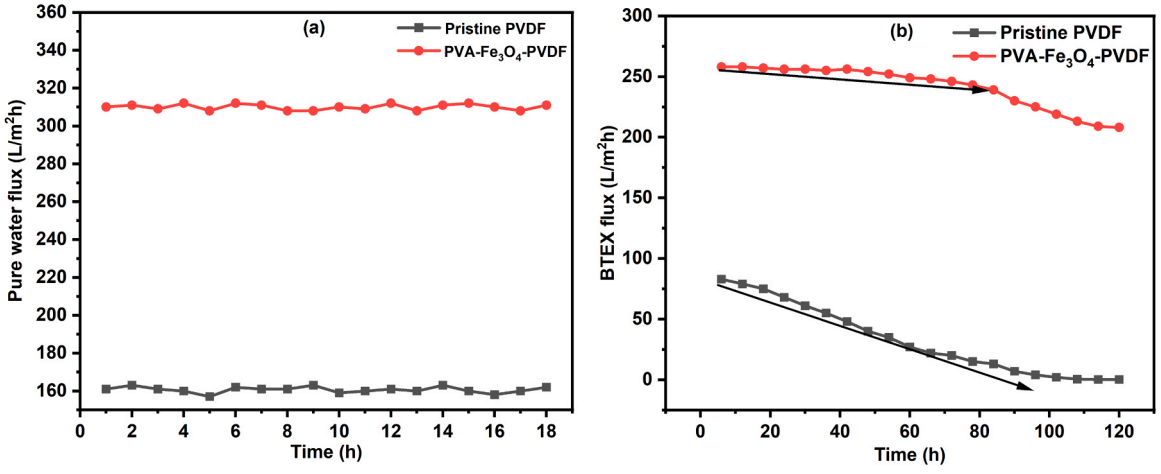

Fig. 9. Variation of (a) PWF and (b) BTEX flux during the long-term filtration tests.

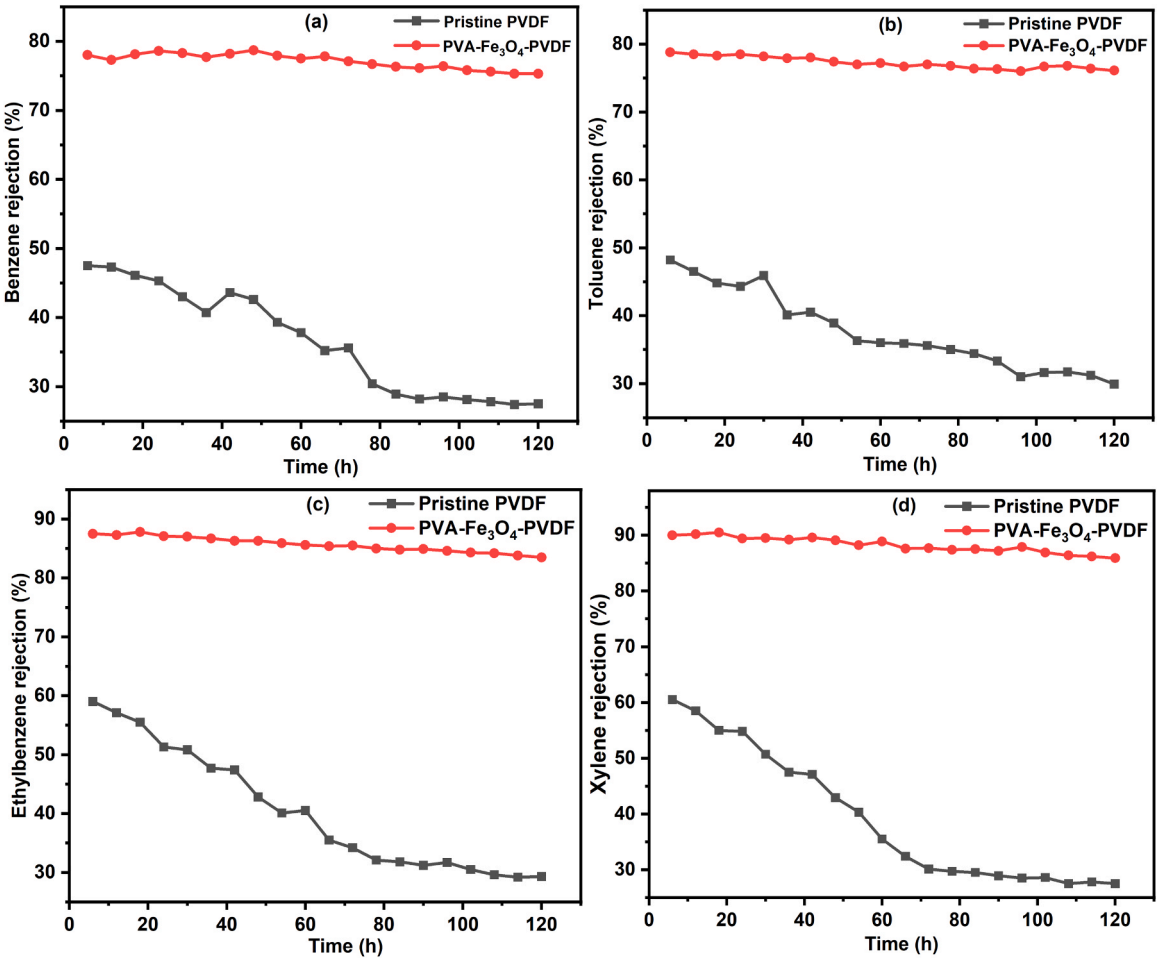

Fig. 10. Variation of the rejection of (a) benzene, (b) toluene, (c) ethylbenzene, and (d) xylene over long-term crossflow filtration.

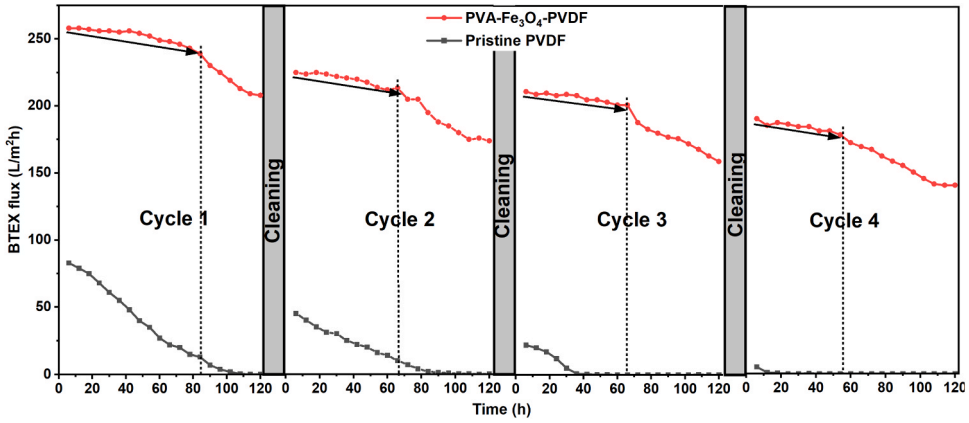

Fig. 11. Reusability of the membrane.

membrane after the long-term filtration test, which shows the presence of the Fe_3O_4-NPs in the membrane matrix, thus indicating that a considerable amount of the NPs remained in the membrane after the long-term filtration test. This further establishes the fairly good stability of the Fe_3O_4-NPs in the membrane.

To assess the stability of the PVA in the membrane matrix, the PVA-Fe_3O_4-PVDF membrane used for the long-term filtration test was thoroughly washed, dried, and analyzed using FTIR to determine its chemical composition. As presented in Fig. 12(b), there was a broad peak at 3369 cm^{-1}, linked to the O-H stretching, confirming the presence of hydrophilic hydroxyl group in the modified membrane. This suggests the presence of PVA in the membrane after the long-term filtration, thus affirming the good stability of the PVA in the membrane matrix.

4. Comparison with similar studies

Table 1 depicts the comparison data of the PVA-Fe_3O_4-PVDF membrane performance with similar reported modified membranes employed for treating BTEX wastewater. Although the operating parameters used in the various studies differ, an idea of the relative

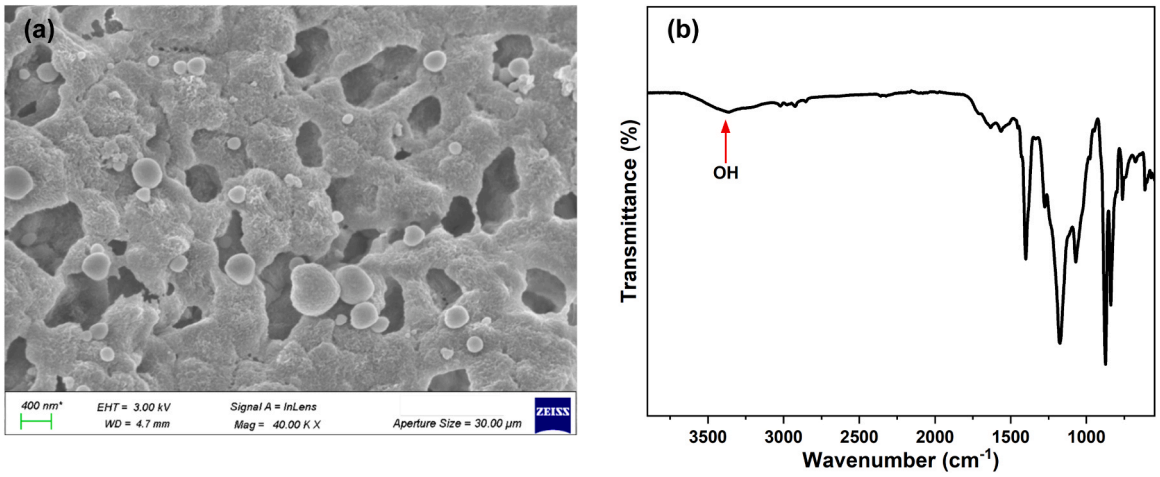

Fig. 12. (a) SEM image, and (b) FTIR spectrum of the PVA-Fe_3O_4-PVDF membrane after long-term filtration test.

Table 1
Comparison of the PVA-Fe_3O_4-PVDF membrane performance with similar reported studies.

Modified membrane	PWF (L/m^{2}h)	R (%)	FRR	Reference
Carbon nanotube/PVDF	7.1	≈ 90 %	-	[74]
Fe-NPs/ PES	84.73	≈ 60 %	-	[51]
TA-Fe^{III}/PES	150.0	≈ 90 %	-	[50]
Fe_3O_4-NPs/PVDF	266.0	≈ 80 %	≈ 80 %	[55]
PVA-Fe_3O_4-PVDF	313.0	≈ 90 %	≈ 98 %	This study

performance of the membranes is outlined. The PVA-Fe_3O_4-PVDF membrane displayed a high PWF compared to the other modified membranes. In addition, the %R and FRR of the PVA-Fe_3O_4-PVDF membrane are comparatively high. Note that the %R described in Table 1 is the reported highest %R of either any of the individual BTEX constituents or all the BTEX components. Summarily, the PVA-Fe_3O_4-PVDF membrane displayed high membrane performance compared to other studies, thereby identifying the modified membrane as a great alternative for the treatment of BTEX wastewater.

5. Conclusion

Hybrid modifiers consisting of Biogenic-synthesized Fe_3O_4-NPs and PVA were used to modify a PVDF membrane to enhance its hydrophilicity and endow the membrane with antifouling ability. Subsequently, the performance of the modified PVA-Fe_3O_4-PVDF membrane was improved, as indicated by its PWF of 313 L/m^{2}h, BTEX flux of 256 L/m^{2}h, and BTEX rejection of approximately 90 %. The membrane also exhibited good operational stability under long-term use, and there was no significant leaching of the incorporated modifiers from the membrane during the filtration tests. In addition, the physical features of the membrane were also improved, as shown by its higher ultimate tensile strength and thermal resistance compared to the pristine PVDF membrane. Overall, the PVA-Fe_3O_4-PVDF membrane displayed enhanced filtration, separation, and antifouling performance, thereby establishing the membrane as a new potential alternative for separating BTEX from contaminated water.

CRediT authorship contribution statement

Michael O. Daramola: Writing – review & editing, Visualization, Validation, Supervision, Software, Project administration, Methodology, Investigation, Formal analysis, Data curation, Conceptualization. **Heidi Richards:** Visualization, Validation, Supervision, Resources, Project administration, Methodology, Investigation, Funding acquisition, Formal analysis, Data curation, Conceptualization. **Ngozi Enemuo:** Writing – review & editing, Writing – original draft, Visualization, Validation, Software, Resources, Project administration, Methodology, Investigation, Funding acquisition, Formal analysis, Data curation, Conceptualization.

Declaration of Competing Interest

The authors declare that they have no known competing financial interests or personal relationships that could have appeared to influence the work reported in this paper.

Data availability

Data will be made available on request.

References

[1] B. Yu, Z. Yuan, Z. Yu, F. Xue-song, BTEX in the environment: an update on sources, fate, distribution, pretreatment, analysis, and removal techniques, Chem. Eng. J. 435 (2022) 134825, https://doi.org/10.1016/j.cej.2022.134825.
[2] S.-T. Lee, C.T. Vu, C. Lin, K.-S. Chen, High occurrence of BTEX around major industrial plants in Kaohsiung, Taiwan, Environ. Forensics 19 (2018) 206–216, https://doi.org/10.1080/15275922.2018.1475432.
[3] A. Liu, N. Hong, P. Zhu, Y. Guan, Understanding benzene series (BTEX) pollutant load characteristics in the urban environment, Sci. Total Environ. 619 (2017) 938–945, https://doi.org/10.1016/j.scitotenv.2017.11.184.
[4] S. Bulatović, M. Ilić, T. Šolević Knudsen, J. Milić, M. Pucarević, B. Jovančićević, M. M. Vrvić, Evaluation of potential human health risks from exposure to volatile organic compounds in contaminated urban groundwater in the Sava river aquifer, Belgrade, Serbia, Environ. Geochem. Health 44 (2022) 3451–3472, https://doi.org/10.1007/s10653-021-01119-2.
[5] L. Ma, A. Hurtado, S. Eguilior, J.F. Llamas Borrajo, Acute and chronic risk assessment of BTEX in the return water of hydraulic fracturing operations in Marcellus Shale, Sci. Total Environ. 906 (2024) 167638, https://doi.org/10.1016/j.scitotenv.2023.167638.
[6] A. Shores, M. Laituri, G. Butters, Produced water surface spills and the risk for btex and naphthalene groundwater contamination, Water Air Soil Pollut. 228 (2017) 435, https://doi.org/10.1007/s11270-017-3618-8.
[7] F. Gissi, J. Strzelecki, M.T. Binet, L.A. Golding, M.S. Adams, T.S. Elsdon, T. Robertson, S.E. Hook, A comparison of short-term and continuous exposures in toxicity tests of produced waters, condensate, and crude oil to marine invertebrates and fish, Environ. Toxicol. Chem. 40 (2021) 2587–2600, https://doi.org/10.1002/etc.5129.
[8] F.A.C. Delunardo, M.G. Paulino, L.C.C. Medeiros, M.N. Fernandes, R. Scherer, A. R. Chippari-Gomes, Morphological and histopathological changes in seahorse (Hippocampus reidi) gills after exposure to the water-accommodated fraction of diesel oil, Mar. Pollut. Bull. 150 (2020) 110769, https://doi.org/10.1016/j.marpolbul.2019.110769.
[9] B.H. Hansen, L. Sørensen, T.R. Størseth, R. Nepstad, D. Altin, D. Krause, S. Meier, T. Nordtug, Embryonic exposure to produced water can cause cardiac toxicity and deformations in Atlantic cod (Gadus morhua) and haddock (Melanogrammus aeglefinus) larvae, Mar. Environ. Res. 148 (2019) 81–86, https://doi.org/10.1016/j.marenvres.2019.05.009.

[10] L.C.C. Medeiros, F.A.C. Delunardo, L.N. Simões, M.G. Paulino, T.S. Vargas, M. N. Fernandes, R. Scherer, A.R. Chippari-Gomes, Water-soluble fraction of petroleum induces genotoxicity and morphological effects in fat snook (Centropomus parallelus, Ecotoxicol. Environ. Saf. 144 (2017) 275–282, https://doi.org/10.1016/j.ecoenv.2017.06.031.
[11] E.R. Rene, M.S. Jo, S.H. Kim, H.S. Park, Statistical analysis of main and interaction effects during the removal of BTEX mixtures in batch conditions, using wastewater treatment plant sludge microbes, Int. J. Environ. Sci. Technol. 4 (2007) 177–182, https://doi.org/10.1007/BF03326271.
[12] C.F. Bustillo-Lecompte, D. Kakar, M. Mehrvar, Photochemical treatment of benzene, toluene, ethylbenzene, and xylenes (BTEX) in aqueous solutions using advanced oxidation processes: towards a cleaner production in the petroleum refining and petrochemical industries, J. Clean. Prod. 186 (2018) 609–617, https://doi.org/10.1016/j.jclepro.2018.03.135.
[13] S. Munirasu, M.A. Haija, F. Banat, Use of membrane technology for oil field and refinery produced water treatment—a review, Process Saf. Environ. Prot. 100 (2016) 183–202, https://doi.org/10.1016/j.psep.2016.01.010.
[14] M. Padaki, R. Surya Murali, M.S. Abdullah, N. Misdan, A. Moslehyani, M. A. Kassim, N. Hilal, A.F. Ismail, Membrane technology enhancement in oil–water separation. A review, Desalination 357 (2015) 197–207, https://doi.org/10.1016/j.desal.2014.11.023.
[15] O. Samuel, M.H.D. Othman, R. Kamaludin, O. Sinsamphanh, H. Abdullah, M. H. Puteh, T.A. Kurniawan, T. Li, A.F. Ismail, M.A. Rahman, J. Jaafar, T. El-badawy, S.C. Mamah, Oilfield-produced water treatment using conventional and membrane-based technologies for beneficial reuse: a critical review, J. Environ. Manag. 308 (2022) 114556, https://doi.org/10.1016/j.jenvman.2022.114556.
[16] S. Alzahrani, A.W. Mohammad, Challenges and trends in membrane technology implementation for produced water treatment: a review, J. Water Process Eng. 4 (2014) 107–133, https://doi.org/10.1016/j.jwpe.2014.09.007.
[17] E. Drioli, A. Ali, Y.M. Lee, S.F. Al-Sharif, M. Al-Beirutty, F. Macedonio, Membrane operations for produced water treatment, Desalin. Water Treat. 57 (2016) 14317–14335, https://doi.org/10.1080/19443994.2015.1072585.
[18] N. Zhang, N. Yang, L. Zhang, B. Jiang, Y. Sun, J. Ma, K. Cheng, F. Peng, Facile hydrophilic modification of PVDF membrane with Ag/EGCG decorated micro/nanostructural surface for efficient oil-in-water emulsion separation, Chem. Eng. J. 402 (2020) 126200, https://doi.org/10.1016/j.cej.2020.126200.
[19] N.H. Ismail, W.N.W. Salleh, A.F. Ismail, H. Hasbullah, N. Yusof, F. Aziz, J. Jaafar, Hydrophilic polymer-based membrane for oily wastewater treatment: a review, Sep. Purif. Technol. 233 (2020) 116007, https://doi.org/10.1016/j.seppur.2019.116007.
[20] S. Kim, K.H. Chu, Y.A.J. Al-Hamadani, C.M. Park, M. Jang, D.-H. Kim, M. Yu, J. Heo, Y. Yoon, Removal of contaminants of emerging concern by membranes in water and wastewater: a review, Chem. Eng. J. 335 (2018) 896–914, https://doi.org/10.1016/j.cej.2017.11.044.
[21] R. Zhang, Y. Liu, M. He, Y. Su, X. Zhao, M. Elimelech, Z. Jiang, Antifouling membranes for sustainable water purification: strategies and mechanisms, Chem. Soc. Rev. 45 (2016) 5888–5924, https://doi.org/10.1039/C5CS00579E.
[22] S.C. Mamah, P.S. Goh, A.F. Ismail, N.D. Suzaimi, L.T. Yogarathinam, Y.O. Raji, T. H. El-badawy, Recent development in modification of polysulfone membrane for water treatment application, J. Water Process Eng. 40 (2021) 101835, https://doi.org/10.1016/j.jwpe.2020.101835.
[23] H.K. Melvin Ng, C.P. Leo, A.Z. Abdullah, Selective removal of dyes by molecular imprinted TiO2 nanoparticles in polysulfone ultrafiltration membrane, J. Environ. Chem. Eng. 5 (2017) 3991–3998, https://doi.org/10.1016/j.jece.2017.07.075.
[24] V. Vatanpour, M. Mehrabi, M. Masteri-Farahani, A.H. Behroozi, M. Niakan, I. Koyuncu, Sulfonic acid functionalized dendrimer-grafted cellulose as a charge and hydrophilic modifier of cellulose acetate membranes in removal of inorganic and organic pollutants, J. Water Process Eng. 50 (2022) 103307, https://doi.org/10.1016/j.jwpe.2022.103307.
[25] Y.H. Kotp, Removal of organic pollutants using polysulfone ultrafiltration membrane containing polystyrene silicomolybdate nanoparticles: case study: Borg El Arab area, J. Water Process Eng. 30 (2019) 100553, https://doi.org/10.1016/j.jwpe.2018.01.008.
[26] A. Suhaimi, E. Mahmoudi, R. Latif, K.S. Siow, M.H.M. Zaid, A.W. Mohammad, M. F. Mohd Razip Wee, Superhydrophilic organosilicon plasma modification on PES membrane for organic dyes filtration, J. Water Process Eng. 44 (2021) 102352, https://doi.org/10.1016/j.jwpe.2021.102352.
[27] Y. Subasi, B. Cicek, Recent advances in hydrophilic modification of PVDF ultrafiltration membranes – a review: part II, Membr. Technol. 2017 (11) (2017) 5, https://doi.org/10.1016/S0958-2118(17)30233-1.
[28] T.D. Kusworo, H. Susanto, N. Aryanti, N. Rokhati, I.N. Widiasa, H. Al-Aziz, D. P. Utomo, D. Masithoh, A.C. Kumoro, Preparation and characterization of photocatalytic PSf-TiO2/GO nanohybrid membrane for the degradation of organic contaminants in natural rubber wastewater, J. Environ. Chem. Eng. 9 (2021) 105066, https://doi.org/10.1016/j.jece.2021.105066.
[29] C.N. Chukwuati, R.M. Moutloali, Antibacterial studies of Ag@HPEI@GO nanocomposites and their effects on fouling and dye rejection in PES UF membranes, Heliyon 8 (2022), https://doi.org/10.1016/j.heliyon.2022.e11825.
[30] L.-P. Zhang, Z. Liu, Y. Faraj, Y. Zhao, R. Zhuang, R. Xie, X.-J. Ju, W. Wang, L.-Y. Chu, High-flux efficient catalytic membranes incorporated with iron-based Fenton-like catalysts for degradation of organic pollutants, J. Membr. Sci. 573 (2019) 493–503, https://doi.org/10.1016/j.memsci.2018.12.032.
[31] Q. Zhong, G. Shi, Q. Sun, P. Mu, J. Li, Robust PVA-GO-TiO2 composite membrane for efficient separation oil-in-water emulsions with stable high flux, J. Membr. Sci. 640 (2021) 119836, https://doi.org/10.1016/j.memsci.2021.119836.
[32] M. Purushothaman, V. Arvind, K. Saikia, V.K. Vaidyanathan, Fabrication of highly permeable and anti-fouling performance of Poly(ether ether sulfone) nanofiltration membranes modified with zinc oxide nanoparticles, Chemosphere 286 (2022) 131616, https://doi.org/10.1016/j.chemosphere.2021.131616.
[33] N. Barati, M.M. Husein, J. Azaiez, Modifying ceramic membranes with in situ grown iron oxide nanoparticles and their use for oily water treatment, J. Membr. Sci. 617 (2021) 118641, https://doi.org/10.1016/j.memsci.2020.118641.
[34] N. Savage, M.S. Diallo, Nanomaterials and water purification: opportunities and challenges, J. Nanopart. Res. 7 (2005) 331–342, https://doi.org/10.1007/s11051-005-7523-5.
[35] Y. Ying, W. Ying, Q. Li, D. Meng, G. Ren, R. Yan, X. Peng, Recent advances of nanomaterial-based membrane for water purification, Appl. Mater. Today 7 (2017) 144–158, https://doi.org/10.1016/j.apmt.2017.02.010.
[36] J. Kim, B. Van der Bruggen, The use of nanoparticles in polymeric and ceramic membrane structures: review of manufacturing procedures and performance improvement for water treatment, Environ. Pollut. 158 (2010) 2335–2349, https://doi.org/10.1016/j.envpol.2010.03.024.
[37] S. Ying, Z. Guan, P.C. Ofoegbu, P. Clubb, C. Rico, F. He, J. Hong, Green synthesis of nanoparticles: current developments and limitations, Environ. Technol. Innov. 26 (2022) 102336, https://doi.org/10.1016/j.eti.2022.102336.
[38] S. Li, X. Huang, Z. Wan, J. Liu, L. Lu, K. Peng, A. Schmidt-Ott, R. Bhattarai, Green synthesis of ultrapure La(OH)3 nanoparticles by one-step method through spark ablation and electrospinning and its application to phosphate removal, Chem. Eng. J. 388 (2020) 124373, https://doi.org/10.1016/j.cej.2020.124373.
[39] J. Qu, Y. Liu, L. Cheng, Z. Jiang, G. Zhang, F. Deng, L. Wang, W. Han, Y. Zhang, Green synthesis of hydrophilic activated carbon supported sulfide nZVI for enhanced Pb(II) scavenging from water: characterization, kinetics, isotherms and mechanisms, J. Hazard. Mater. 403 (2021) 123607, https://doi.org/10.1016/j.jhazmat.2020.123607.
[40] Y.-C. Lin, H.-H. Tseng, D.K. Wang, Uncovering the effects of PEG porogen molecular weight and concentration on ultrafiltration membrane properties and protein purification performance, J. Membr. Sci. 618 (2021) 118729, https://doi.org/10.1016/j.memsci.2020.118729.
[41] F. Yalcinkaya, A. Siekierka, M. Bryjak, Surface modification of electrospun nanofibrous membranes for oily wastewater separation, RSC Adv. 7 (2017) 56704–56712, https://doi.org/10.1039/C7RA11904F.
[42] Q. Lu, N. Li, X. Zhang, Supramolecular recognition PVDF/PVA ultrafiltration membrane for rapid removing aromatic compounds from water, Chem. Eng. J. 436 (2022) 132889, https://doi.org/10.1016/j.cej.2021.132889.
[43] J. Zhang, Q. Wang, Z. Wang, C. Zhu, Z. Wu, Modification of poly(vinylidene fluoride)/polyethersulfone blend membrane with polyvinyl alcohol for improving antifouling ability, J. Membr. Sci. 466 (2014) 293–301, https://doi.org/10.1016/j.memsci.2014.05.006.
[44] S. Amiri, A. Asghari, A.R. Harifi-Mood, M. Rajabi, T. He, V. Vatanpour, Polyvinyl alcohol and sodium alginate hydrogel coating with different crosslinking procedures on a PSf support for fabricating high-flux NF membranes, Chemosphere 308 (2022) 136323, https://doi.org/10.1016/j.chemosphere.2022.136323.
[45] Y. Sun, Y. Zong, N. Yang, N. Zhang, B. Jiang, L. Zhang, X. Xiao, Surface hydrophilic modification of PVDF membranes based on tannin and zwitterionic substance towards effective oil-in-water emulsion separation, Sep. Purif. Technol. 234 (2020) 116015, https://doi.org/10.1016/j.seppur.2019.116015.
[46] Z.C. Ng, W.J. Lau, A.F. Ismail, GO/PVA-integrated TFN RO membrane: exploring the effect of orientation switching between PA and GO/PVA and evaluating the GO loading impact, Desalination 496 (2020) 114538, https://doi.org/10.1016/j.desal.2020.114538.
[47] C. Zuo, L. Wang, Y. Tong, L. Shi, W. Ding, W. Li, Co-deposition of pyrogallol/polyethyleneimine on polymer membranes for highly efficient treatment of oil-in-water emulsion, Sep. Purif. Technol. 267 (2021) 118660, https://doi.org/10.1016/j.seppur.2021.118660.
[48] H. Liu, H. Yu, X. Yuan, W. Ding, Y. Li, J. Wang, Amino-functionalized mesoporous PVA/SiO2 hybrids coated membrane for simultaneous removal of oils and water-soluble contaminants from emulsion, Chem. Eng. J. 374 (2019) 1394–1402, https://doi.org/10.1016/j.cej.2019.05.161.
[49] A. Saeedi-Jurkuyeh, A. Jonidi Jafari, R.R. Kalantary, A. Esrafili, Preparation of a thin-film nanocomposite forward osmosis membrane for the removal of organic micro-pollutants from aqueous solutions, Environ. Technol. 42 (2021) 3011–3024, https://doi.org/10.1080/09593330.2020.1720307.
[50] T. Makhani, O.O. Sadare, S. Wagenaar, K. Moothi, R.M. Moutloali, M.O. Daramola, Fabrication and performance evaluation of tannin iron complex (TA-FeIII/PES) UF membrane in treatment of BTEX wastewater, Water SA 48 (2022) 457–466.
[51] C.F. Unuigbe, O.M. Fayemiwo, M.O. Daramola, Performance evaluation of iron nanoparticles infused polyethersulphone (Fe-NPs/PES) membrane during treatment of BTEX-contaminated wastewater, Water Environ. J. 34 (2020) 74–86, https://doi.org/10.1111/wej.12506.
[52] N. Ghaemi, S.S. Madaeni, P. Daraei, H. Rajabi, S. Zinadini, A. Alizadeh, R. Heydari, M. Beygzadeh, S. Ghouzivand, Polyethersulfone membrane enhanced with iron oxide nanoparticles for copper removal from water: application of new functionalized Fe_3O_4 nanoparticles, Chem. Eng. J. 263 (2015) 101–112, https://doi.org/10.1016/j.cej.2014.10.103.
[53] M. Martínez-Cabanas, M. López-García, J.L. Barriada, R. Herrero, M.E. Sastre de Vicente, Green synthesis of iron oxide nanoparticles. Development of magnetic hybrid materials for efficient As(V) removal, Chem. Eng. J. 301 (2016) 83–91, https://doi.org/10.1016/j.cej.2016.04.149.
[54] J. Zhang, Z. Wang, Q. Wang, J. Ma, J. Cao, W. Hu, Z. Wu, Relationship between polymers compatibility and casting solution stability in fabricating PVDF/PVA

membranes, J. Membr. Sci. 537 (2017) 263–271, https://doi.org/10.1016/j.memsci.2017.05.041.
[55] N. Enemuo, H. Richards, M.O. Daramola, Evaluation of the performance of Fe_3O_4-NPs/PVDF nanocomposite membrane for removal of BTEX from contaminated water, J. Water Process Eng. 60 (2024) 105185, https://doi.org/10.1016/j.jwpe.2024.105185.
[56] J. Zhang, Z. Wang, Q. Wang, J. Ma, J. Cao, W. Hu, Z. Wu, Relationship between polymers compatibility and casting solution stability in fabricating PVDF/PVA membranes, J. Membr. Sci. 537 (2017) 263–271, https://doi.org/10.1016/j.memsci.2017.05.041.
[57] H. Ju, A.C. Sagle, B.D. Freeman, J.I. Mardel, A.J. Hill, Characterization of sodium chloride and water transport in crosslinked poly(ethylene oxide) hydrogels, J. Membr. Sci. 358 (2010) 131–141, https://doi.org/10.1016/j.memsci.2010.04.035.
[58] D.F. Leusch, D.M. Bartkow. A Short Primer on Benzene, Toluene, Ethylbenzene and Xylenes (BTEX) in the Environment and in Hydraulic Fracturing Fluids, Griffith University, 2010.
[59] R. Mukherjee, S. De, Novel carbon-nanoparticle polysulfone hollow fiber mixed matrix ultrafiltration membrane: adsorptive removal of benzene, phenol and toluene from aqueous solution, Sep. Purif. Technol. 157 (2016) 229–240, https://doi.org/10.1016/j.seppur.2015.11.015.
[60] T.D. Kusworo, M. Yulfarida, A.C. Kumoro, S. Sumardiono, M. Djaeni, T. A. Kurniawan, M.H.D. Othman, B. Budiyono, A highly durable and hydrophilic PVDF- MoS2/WO3-PVA membrane with visible light driven self-cleaning performance for pollutant-burdened natural rubber wastewater treatment, J. Environ. Chem. Eng. 11 (2023) 109583, https://doi.org/10.1016/j.jece.2023.109583.
[61] S. Sakarkar, S. Muthukumaran, V. Jegatheesan, Evaluation of polyvinyl alcohol (PVA) loading in the PVA/titanium dioxide (TiO2) thin film coating on polyvinylidene fluoride (PVDF) membrane for the removal of textile dyes, Chemosphere 257 (2020) 127144, https://doi.org/10.1016/j.chemosphere.2020.127144.
[62] Q. Lu, X. Zhang, N. Hing Wong, J. Sunarso, N. Li, Anti-biofouling polyvinylidene fluoride/quaternized polyvinyl alcohol ultrafiltration membrane selectively separates aromatic contaminants from wastewater by host–guest interactions, Sep. Purif. Technol. 296 (2022) 121387, https://doi.org/10.1016/j.seppur.2022.121387.
[63] I. Deleanu, A.M.S. Stoica, L. Dobre, T. Dobre, S. Jinga, C. Tardei, Potassium sorbate release from poly(vinyl alcohol)–bacterial cellulose films, Chem. Pap. 66 (2012) 138–143, https://doi.org/10.2478/s11696-011-0068-4.
[64] L. Zheng, M. Tang, Y. Wang, D. Hou, X. Li, J. Wang, A novel Cu-BTC@PVA/PVDF Janus membrane with underwater-oleophobic/hydrophobic asymmetric wettability for anti-fouling membrane distillation, Sep. Purif. Technol. 299 (2022) 121807, https://doi.org/10.1016/j.seppur.2022.121807.
[65] L.Y. Ng, A.W. Mohammad, C.P. Leo, N. Hilal, Polymeric membranes incorporated with metal/metal oxide nanoparticles: a comprehensive review, Desalination 308 (2013) 15–33, https://doi.org/10.1016/j.desal.2010.11.033.
[66] C. Liu, Y. Guo, Y. Zhou, B. Yang, K. Xiao, H.-Z. Zhao, High-hydrophilic and antifouling reverse osmosis membrane prepared based an unconventional radiation method for pharmaceutical plant effluent treatment, Sep. Purif. Technol. 280 (2022) 119838, https://doi.org/10.1016/j.seppur.2021.119838.
[67] S. Zarghami, T. Mohammadi, M. Sadrzadeh, B. Van der Bruggen, Superhydrophilic and underwater superoleophobic membranes - a review of synthesis methods, Prog. Polym. Sci. 98 (2019) 101166, https://doi.org/10.1016/j.progpolymsci.2019.101166.
[68] J. Gu, L. Ji, P. Xiao, C. Zhang, J. Li, L. Yan, T. Chen, Recent progress in superhydrophilic carbon-based composite membranes for oil/water emulsion separation, ACS Appl. Mater. Interfaces 13 (2021) 36679–36696, https://doi.org/10.1021/acsami.1c07737.
[69] X. Zhao, R. Zhang, Y. Liu, M. He, Y. Su, C. Gao, Z. Jiang, Antifouling membrane surface construction: chemistry plays a critical role, J. Membr. Sci. 551 (2018) 145–171, https://doi.org/10.1016/j.memsci.2018.01.039.
[70] B. Saini, D. Vaghani, S. Khuntia, M.K. Sinha, A. Patel, R. Pindoria, A novel stimuli-responsive and fouling resistant PVDF ultrafiltration membrane prepared by using amphiphilic copolymer of poly(vinylidene fluoride) and Poly(2-N-morpholino) ethyl methacrylate, J. Membr. Sci. 603 (2020) 118047, https://doi.org/10.1016/j.memsci.2020.118047.
[71] P.M. Williams, Membrane charge (Zeta Potential) Effect, in: E. Drioli, L. Giorno (Eds.), Encyclopedia of Membranes, Springer, Berlin, 2016, pp. 1–2, https://doi.org/10.1007/978-3-642-40872-4_1003-1.
[72] A.E. Childress, M. Elimelech, Relating nanofiltration membrane performance to membrane charge (electrokinetic) characteristics, Environ. Sci. Technol. 34 (2000) 3710–3716, https://doi.org/10.1021/es0008620.
[73] Z. Xiong, J. Liu, Y. Yang, Q. Lai, X. Wu, J. Yang, Q. Zeng, G. Zhang, S. Zhao, Reinforcing hydration layer on membrane surface via nano-capturing and hydrothermal crosslinking for fouling reduction, J. Membr. Sci. 644 (2022) 120076, https://doi.org/10.1016/j.memsci.2021.120076.
[74] F. Su, C. Lu, J.-H. Tai, Separation of benzene, toluene, ethylbenzene and p-xylene from aqueous solutions by carbon nanotubes/polyvinylidene fluoride nanocomposite membrane, J. Water Resour. Prot. 8 (10) (2016), https://doi.org/10.4236/jwarp.2016.810075.
[75] Y.H. Tan, P.S. Goh, A.F. Ismail, B.C. Ng, G.S. Lai, Decolourization of aerobically treated palm oil mill effluent (AT-POME) using polyvinylidene fluoride (PVDF) ultrafiltration membrane incorporated with coupled zinc-iron oxide nanoparticles, Chem. Eng. J. 308 (2017) 359–369, https://doi.org/10.1016/j.cej.2016.09.092.
[76] M.R. Esfahani, S.A. Aktij, Z. Dabaghian, M.D. Firouzjaei, A. Rahimpour, J. Eke, I. C. Escobar, M. Abolhassani, L.F. Greenlee, A.R. Esfahani, A. Sadmani, N. Koutahzadeh, Nanocomposite membranes for water separation and purification: fabrication, modification, and applications, Sep. Purif. Technol. 213 (2019) 465–499, https://doi.org/10.1016/j.seppur.2018.12.050.
[77] WHO, Guidelines for drinking-water quality: incorporating the 1st addendum. ⟨https://www.who.int/publications-detail-redirect/9789241549950⟩ (Accessed 18 December 2023).